Electronic Supplementary Material (ESI) for Journal of Materials Chemistry A.


# Supporting Information

## Mesoporous Single-Crystalline $MnO_x$ Nanofibers@Graphene for Ultra-High Rate and Long-Life Lithium-Ion Battery Anodes

*Chenglong Xu† [a], Zheng Liu† [a], Tong Wei* [a], Lizhi Sheng [a], Longhai Zhang [a], Lan Chen [a], Qihang Zhou [a], Zimu Jiang [a], Lin Wang* [b] and Zhuangjun Fan* [a,b]*

a. Key Laboratory of Superlight Materials and Surface Technology, Ministry of Education, College of Material Science and Chemical Engineering, Harbin Engineering University, Harbin 150001, China

b. School of Material Science and Engineering, China University of Petroleum, Qingdao 266580, China

E-mail: weitong666@163.com; linwangsxh@hotmail.com; fanzhj666@163.com

*† These authors contributed equally to this work.*

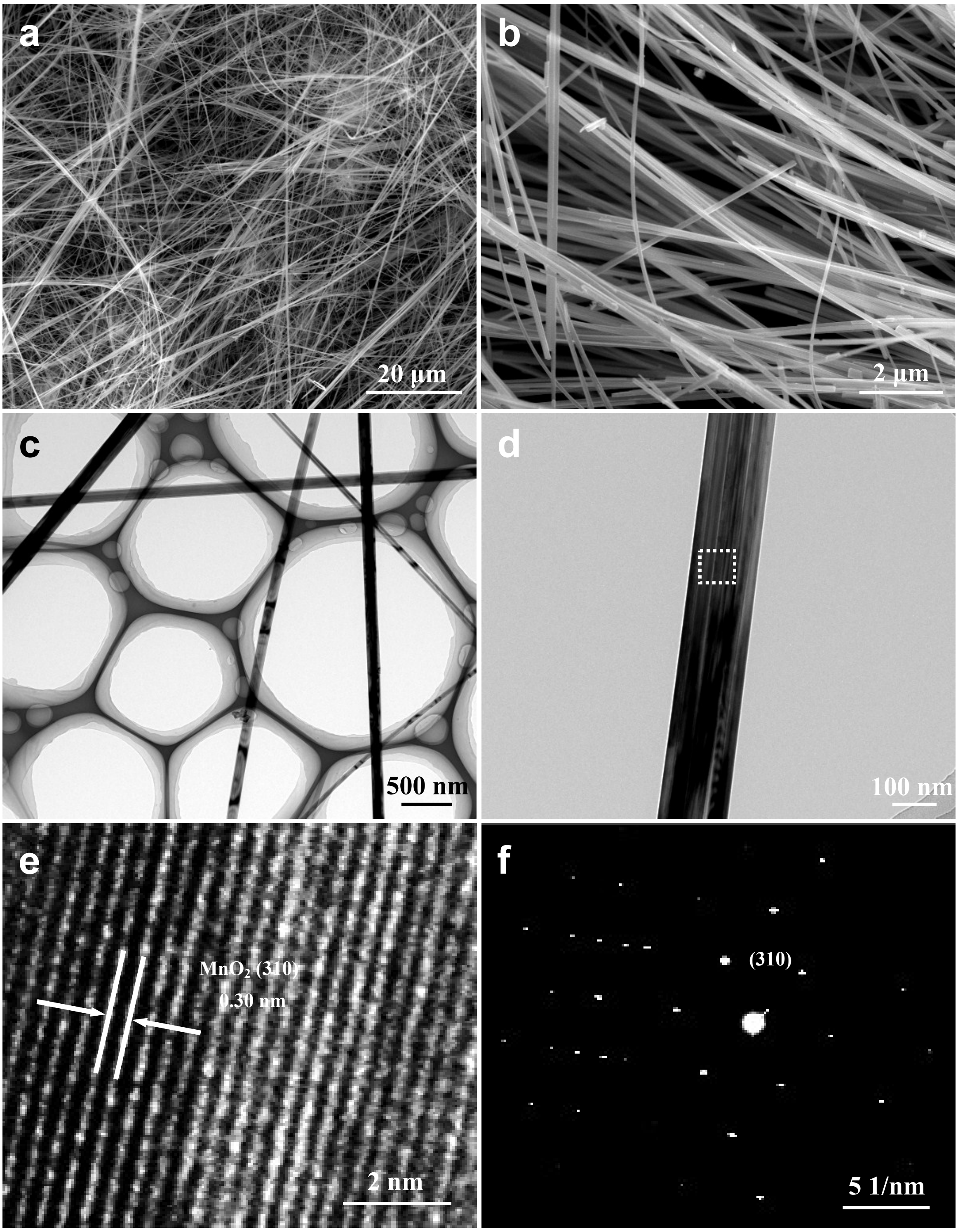


**Fig. S1.** (a,b) SEM images of the as-prepared $MnO_2$ NFs. (c,d) TEM images of $MnO_2$ NFs. (e,f) The high resolution TEM (HRTEM) image and selected area diffraction (SAED) pattern of $MnO_2$ NFs.

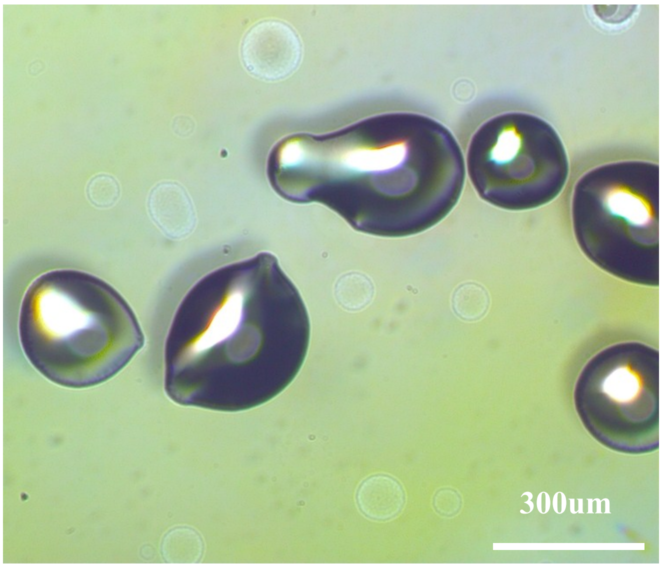


**Fig. S2.** Polarized optical microscope (POM) image of micro-sized droplets of $MnO_2$ NFs/GO suspension.

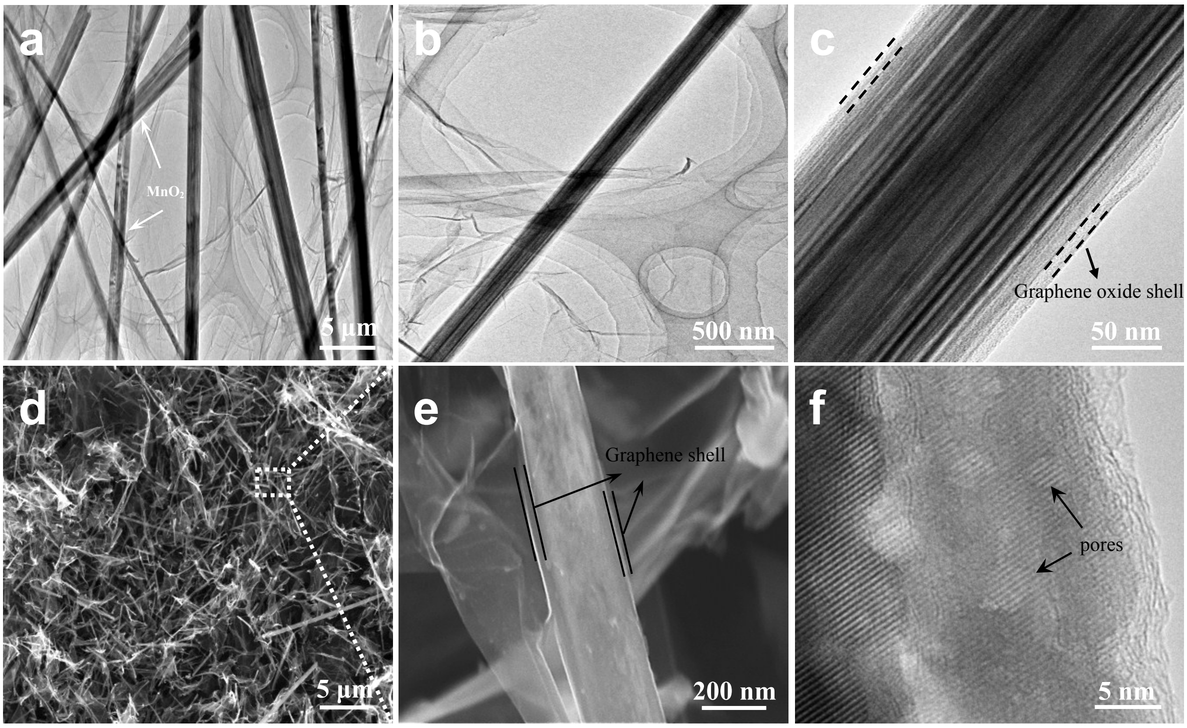


**Fig. S3.** (a,b,c) TEM images of $SCMnO_2$@GO. (d,e) SEM images and (f) HRTEM image of $PSCMnO_x$@G.

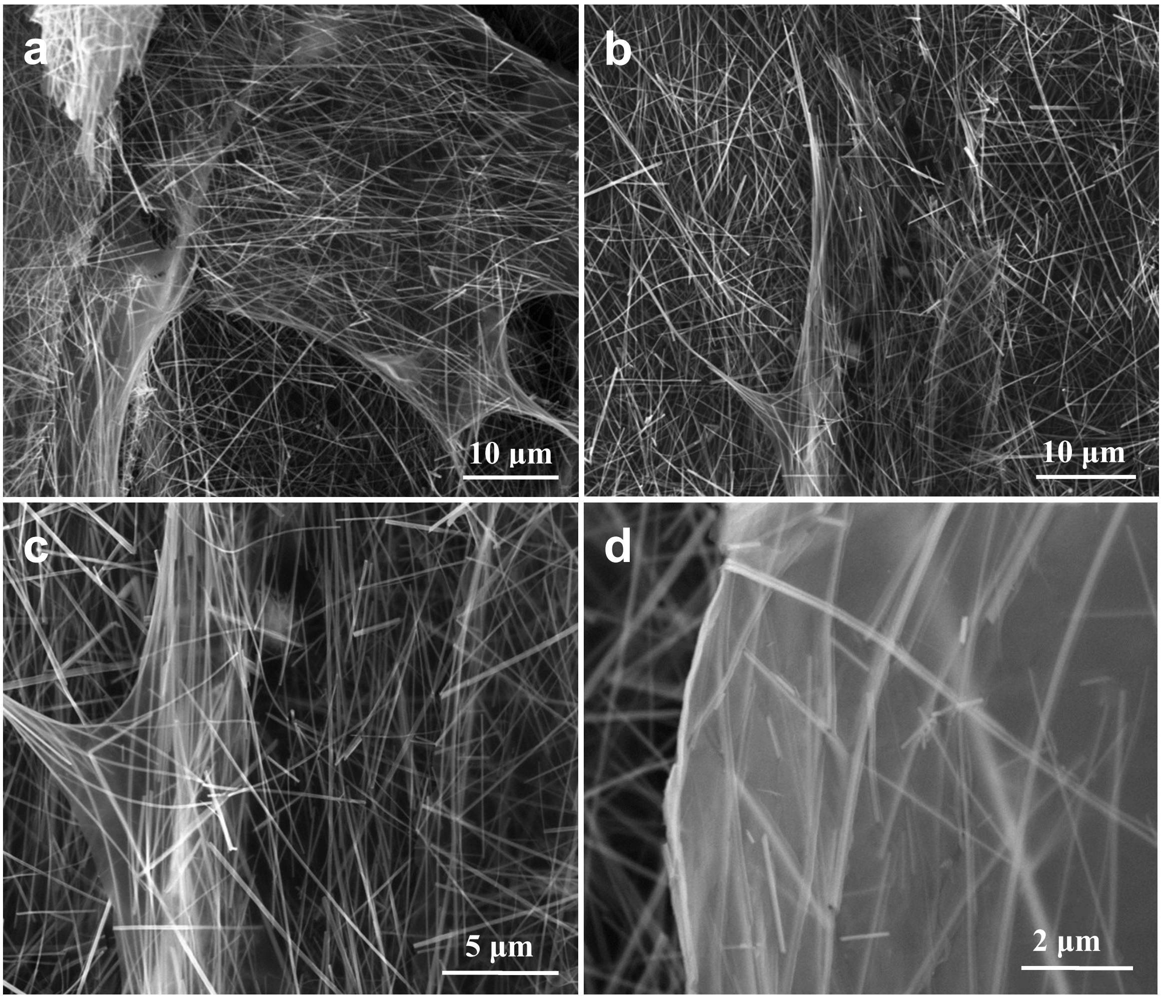


**Fig. S4.** SEM images of $MnO_2$/GO at different magnifications.

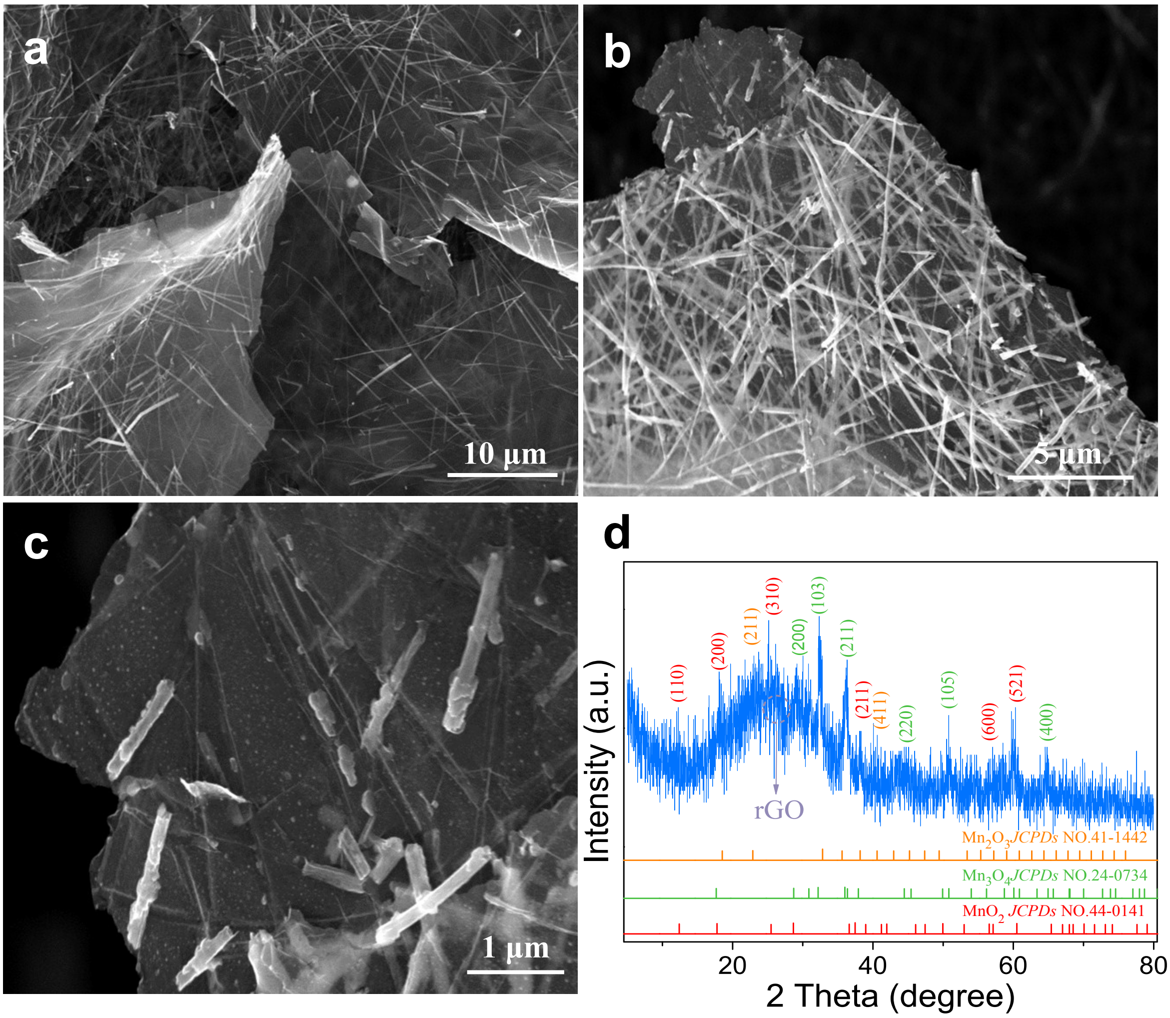


**Fig. S5.** (a-c) SEM images of $MnO_x$/G at different magnifications. (d) XRD pattern of $MnO_x$/G.

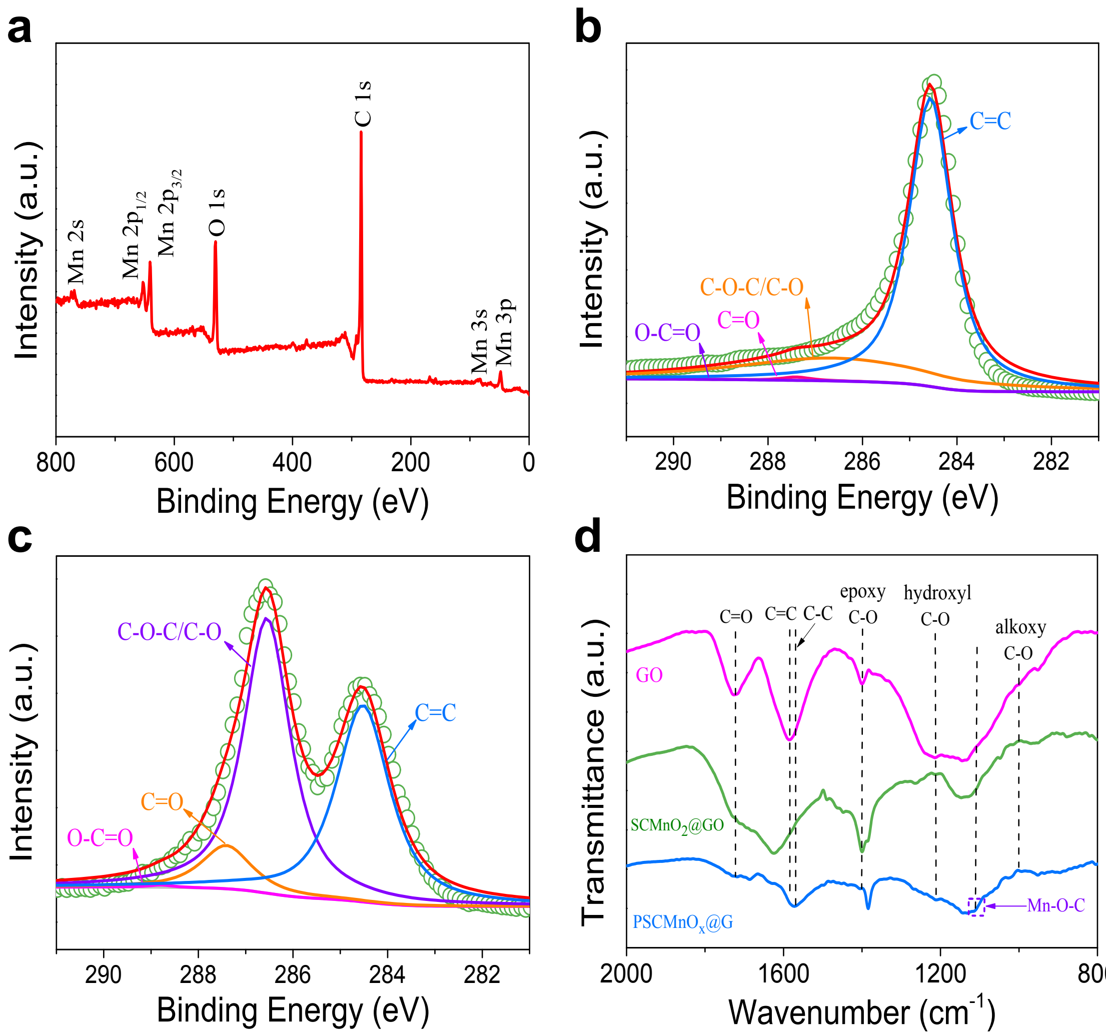


**Fig. S6.** (a) XPS survey spectrum and (b) high-resolution C 1s XPS spectra of PSCMnO$_x$@G. (c) High-resolution C 1s XPS spectra of SCMnO$_2$@GO. (d) FTIR spectra of PSCMnO$_x$@G, SCMnO$_2$@GO and GO.

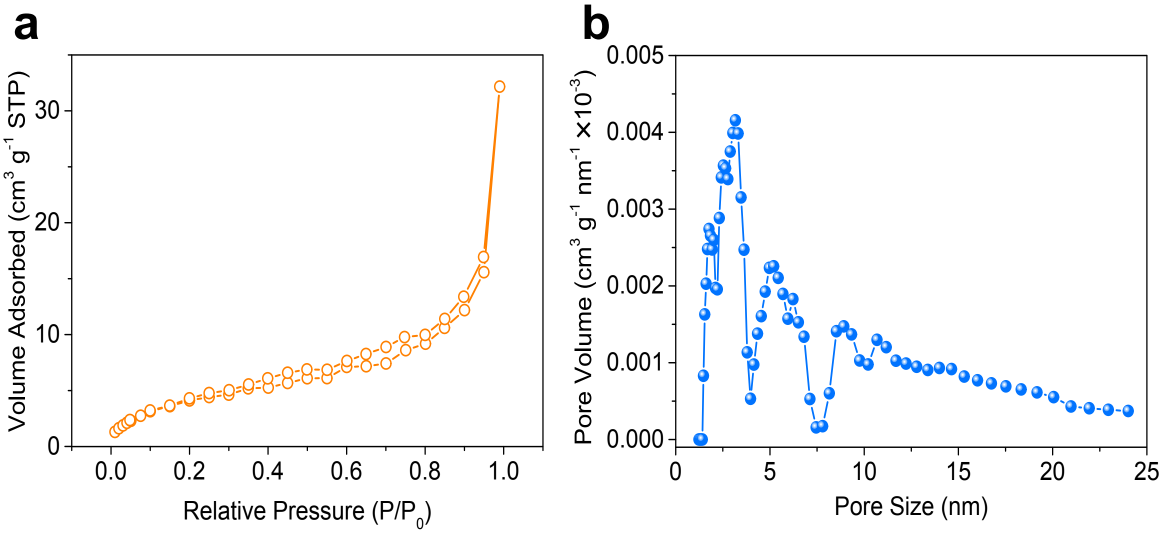


**Fig. S7.** (a) Nitrogen adsorption and desorption isotherm and (b) pore-size distribution plot of pristine $MnO_2$.

**Table S1**. Specific surface area obtained from $N_2$ adsorption/desorption test.

| **Samples** | Specific surface area $m^2$ $g^{-1}$ | Micropore area $m^2$ $g^{-1}$ | Mesopore area $m^2$ $g^{-1}$ |
|---|---|---|---|
| Pristine $MnO_2$ | 16.2 | 1.5 | 11.3 |
| $SCMnO_2$@GO | 31.9 | 1.2 | 30.6 |
| $PSCMnO_x$@G | 58.8 | 8.5 | 50.3 |

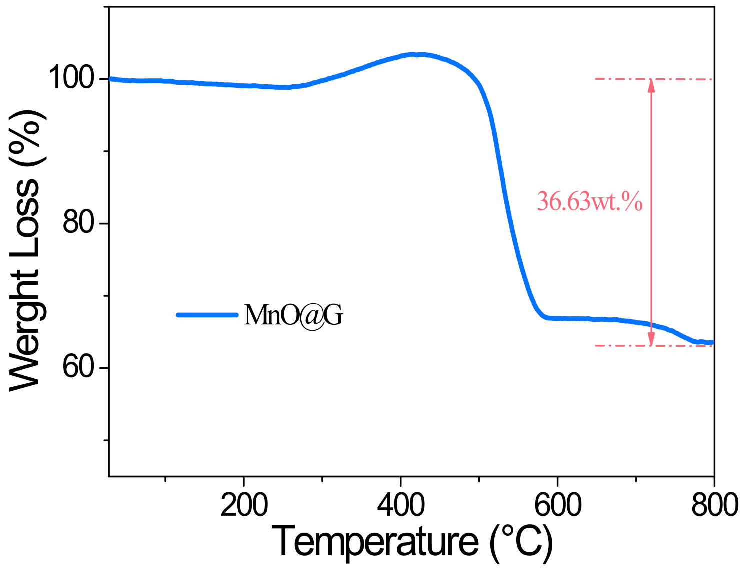


**Fig. S8.** TGA curve of MnO@G. The SCMnO$_2$@GO was annealed at 800 °C under a hydrogen atmosphere for 2 h to obtain the MnO@G. The content of graphene in MnO@G is the same as in PSCMnO$_x$@G. The final product of MnO@G after annealing at 800 ºC in air can be assigned to the tetragonal structure of $Mn_3O_4$ phase, indicating that the MnO was oxidized to $Mn_3O_4$. In theory, this oxidation process will give rise to a 7.5wt.% weight increase. Assuming that the total mass is 1 and the carbon content is x, then the MnO content is (1-x). As shown in the TGA curve, the weight loss can be calculated using the following formula: x-7.5 wt.%(1-x) = 36.63 wt.%. Thus, the carbon content x is equal to 41.05wt%.

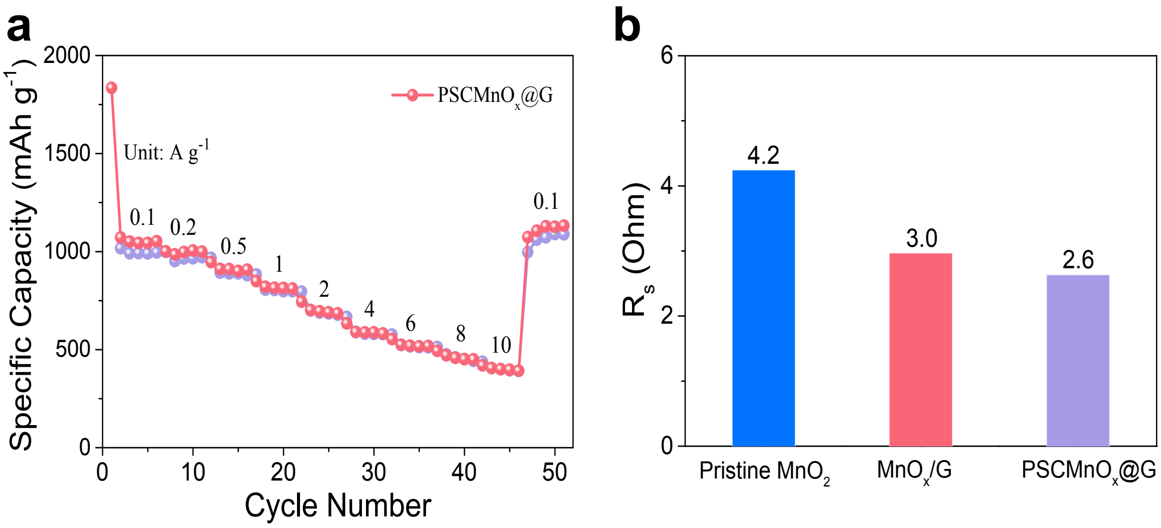


**Fig. S9.** (a) Rate capabilities of PSCMnO$_x$@G at the current densities from 0.1 to 10.0 A g$^{-1}$. (b) The R$_s$ of the PSCMnOx@G, MnOx/G and pristine MnO2 electrodes.

**Table S2**. Comparison of the electrochemical performance of $PSCMnO_x@G$ with previously reported $MnO_x$ based electrodes.

| Manganese oxide -based materials | Rate performance [ mA h $g^{-1}$] | Cycling performance [mA h $g^{-1}$] | Ref. |
|---|---|---|---|
| GNS@MnO@N-C | 873 (0.1 A $g^{-1}$); 165 (2.0A $g^{-1}$) | 754 (0.1 A $g^{-1}$, 350 cycles) | [19] |
| α-$Mn_2O_3$ nanocrystals | 780 (0.1 A $g^{-1}$); 425(3.2 A $g^{-1}$) | 780 (0.1A $g^{-1}$, 100 cycles) | [23] |
| Carbon NFs/MnO | 1006 (0.1 A $g^{-1}$); 409 (2.0 A $g^{-1}$) | 992 (0.2 A $g^{-1}$, 50 cycles) | [8] |
| $MnCO_3/Mn_3O_4$/RGO | 800 (0.1 A $g^{-1}$); 150 (3.2 A $g^{-1}$) | 532 (1.0 A $g^{-1}$, 800 cycles) | [17] |
| MnO/C nanopeapods | 845 (0.1 A $g^{-1}$); 320 (5.0 A $g^{-1}$) | 525 (2.0 A $g^{-1}$, 1000 cycles) | [25] |
| Coaxial MnO/N-C nanorods | 828 (0.2 A $g^{-1}$); 372 (5.0 A $g^{-1}$) | 982 (0.5 A $g^{-1}$, 100 cycles) | [34] |
| MnO@$Mn_3O_4$/NPCF | 660 (0.2 A $g^{-1}$); 280 (2.0 A $g^{-1}$) | 1500 (0.2 A $g^{-1}$, 270 cycles) | [14] |
| GO-$MnO_2$-GO NRBs | 680 (0.1 A $g^{-1}$); 280 (2.0 A $g^{-1}$) | 612 (0.4 A $g^{-1}$, 250 cycles) | [9] |
| $MnO_2$/RGO | 964 (0.1 A $g^{-1}$); 115 (10 A $g^{-1}$) | 1574 (1.0 A $g^{-1}$, 500 cycles) | [10] |
| $MnO_x$/SWCNT | 866 (0.2 A $g^{-1}$); 437 (0.8 A $g^{-1}$) | 850 (0.1 A $g^{-1}$, 36 cycles) | [28] |
| MnNCN | 792 (0.1 A $g^{-1}$); 320 (3.2 A $g^{-1}$) | 385 (5.0 A $g^{-1}$, 500 cycles) | [16] |
| MnO@N-C | 1097 (0.1 A $g^{-1}$); 438 (2.0 A $g^{-1}$) | 690 (1.0 A $g^{-1}$, 150 cycles) | [15] |
| MnO@CF | 895 (0.2 A $g^{-1}$); 513 (4.0 A $g^{-1}$) | 1040 (0.2 A $g^{-1}$, 500 cycles) | [42] |
| G/MnO-800 | 1000 (0.1 A $g^{-1}$); 270 (8.0 A $g^{-1}$) | 620 (1.0 A $g^{-1}$, 600 cycles) | [29] |
| MnO@C CSNWs | 880 (0.1 A $g^{-1}$); 356 (5.0 A $g^{-1}$) | 750 (1.0 A $g^{-1}$, 200 cycles) | [18] |
| $Mn_3O_4$/N-C fiber | 1058 (0.05 A $g^{-1}$); 320 (2.5 A $g^{-1}$) | 1007 (0.1 A $g^{-1}$, 160 cycles) | [26] |
| MnO nanowires/graphene | 780 (0.05 A $g^{-1}$); 300 (1.0 A $g^{-1}$) | 930 (0.5 A $g^{-1}$, 500 cycles) | [33] |
| **$PSCMnO_x@G$** | **1072 (0.1 A $g^{-1}$); 420 (10 A $g^{-1}$)** | **1163 (2.0 A $g^{-1}$, 500 cycles)** | **This work** |

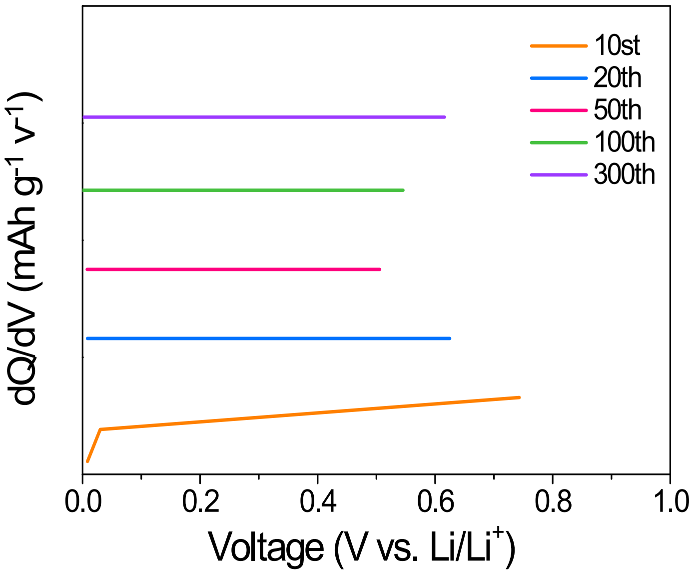


**Fig. S10.** Differential capacities (dQ/dV) versus voltage plots of pristine $MnO_2$ for different cycles at 2.0 A $g^{-1}$.

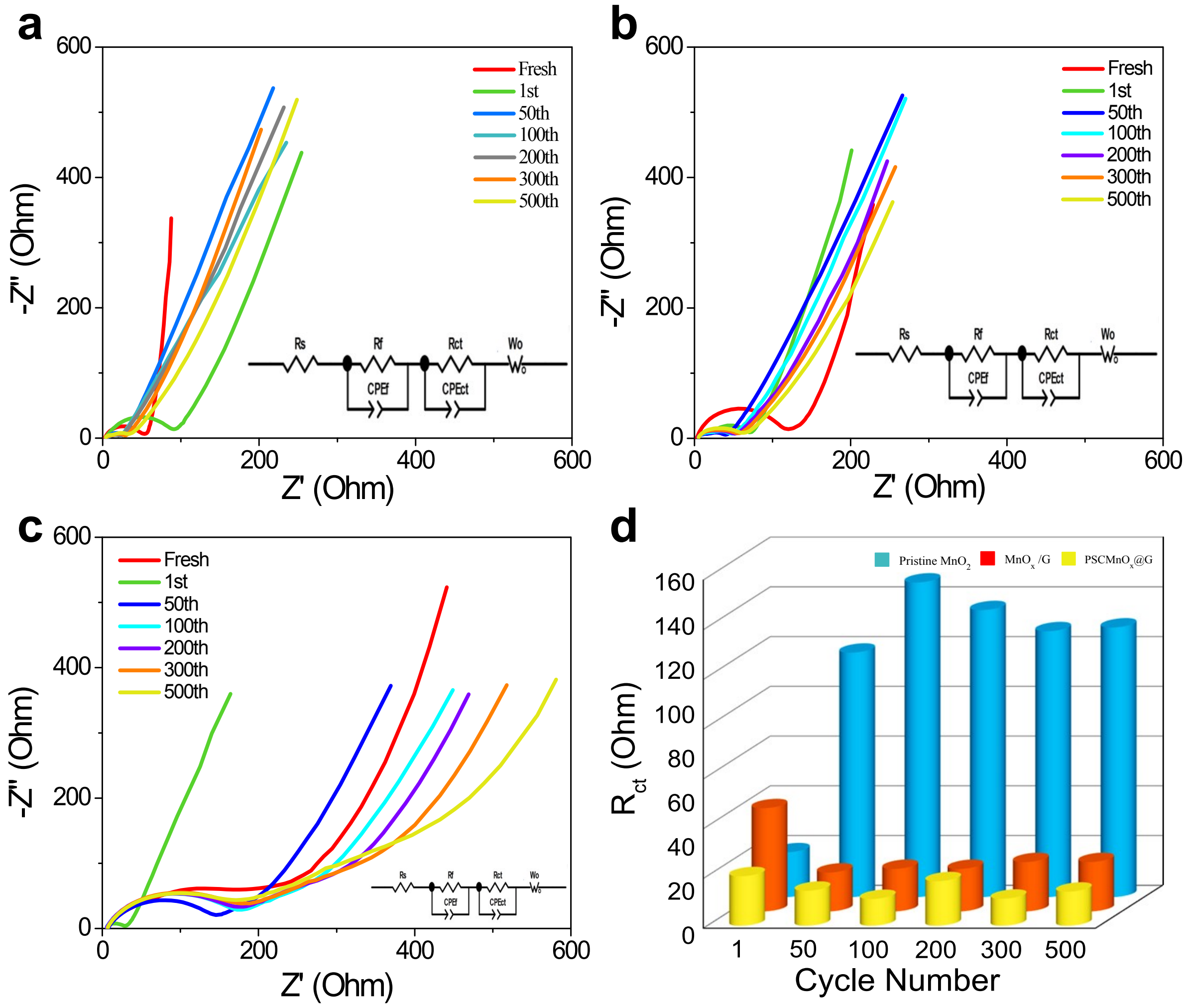


**Fig. S11.** Nyquist impendence plots of (a) PSCMnO$_x$@G, (b) MnO$_x$/G and (c) pristine MnO$_2$ for different cycles at 2.0 A g$^{-1}$. (d) R$_{ct}$ of PSCMnO$_x$@G, MnO$_x$/G and pristine MnO$_2$ for different cycles at 2.0 A g$^{-1}$.

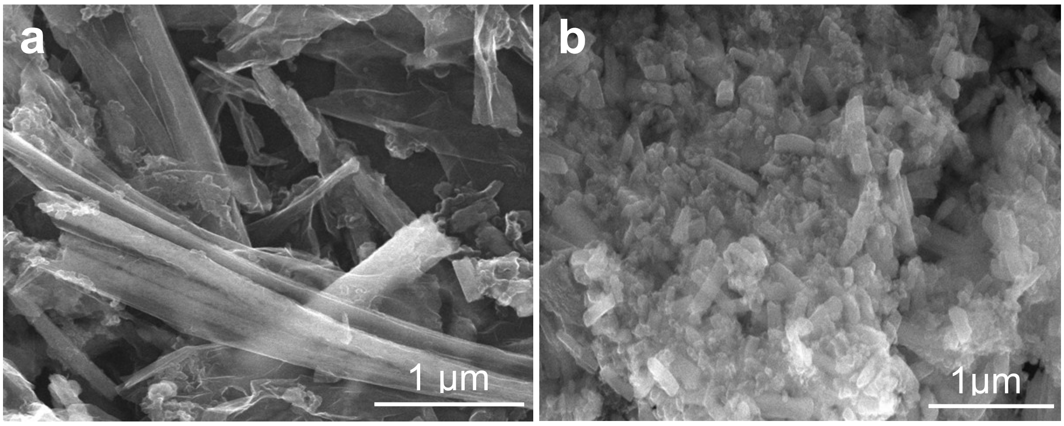


**Fig. S12.** SEM images of (a) the PSCMnO$_x$@G and (b) $MnO_2$ nanofibers after 500 cycles at 2.0 A g$^{-1}$.